Hydrol. Earth Syst. Sci. Discuss., 8, 2699–2738, 2011
www.hydrol-earth-syst-sci-discuss.net/8/2699/2011/
doi:10.5194/hessd-8-2699-2011

Hydrology and Earth System Sciences Discussions

Combining flow routing modelling and direct velocity measurement for optimal discharge estimation

G. Corato[1], **T. Moramarco**[1], **and T. Tucciarelli**[2]

[1]Research Institute for Hydro-geological Protection, National Research Council, via della Madonna Alta, 126, 06128, Perugia, Italy
[2]Department of Civil, Environmental and Aerospace Engineering , University of Palermo, Italy, Viale delle Scienze, 90128, Palermo, Italy

Received: 1 March 2011 – Accepted: 8 March 2011 – Published: 10 March 2011

Correspondence to: G. Corato (g.corato@irpi.cnr.it)

Published by Copernicus Publications on behalf of the European Geosciences Union.

Abstract

A new procedure is proposed for estimating river discharge hydrographs during flood events, using only water level data measured at a gauged site, as well as 1-D shallow water modelling and sporadic maximum surface flow velocity measurements. During flood, the piezometric level is surmised constant in the vertical plane of the river section, where the top of the banks is always above the river level, and is well represented by the recorded stage hydrograph. The river is modelled along the reach directly located downstream the upstream gauged section, where discharge hydrograph is sought after. For the stability with respect to the topographic error, as well as for the simplicity of the data required to satisfy the boundary conditions, a diffusive hydraulic model is adopted for flow routing. Assigned boundary conditions are: (1) the recorded stage hydrograph at the upstream river site and (2) the zero diffusion condition at the downstream end of the reach. The MAST algorithm is used for the numerical solution of the flow routing problem, which is embedded in the Brent algorithm used for the computation of the optimum Manning coefficient. Based on synthetic tests concerning a broad prismatic channel, the optimal reach length is chosen so that the approximated downstream boundary condition effects on discharge hydrograph assessment at upstream end are negligible. The roughness Manning coefficient is calibrated by using sporadic instantaneous surface velocity measurements during the rising limb of flood that are turned into instantaneous discharges through the solid of velocity estimated by a two-dimensional entropic model. Several historical events, occurring in three gauged sites along the upper Tiber River wherein a reliable rating curve is available, have been used for the validation. The analysis outcomes can be so summarized: (1) criteria adopted for selecting the optimal channel length and based on synthetic tests have been proved reliable by using field data of three gauged river sites. Indeed, for each of them a downstream reach, long not more than 500 m, is turned out fair for achieving good performances of the diffusive hydraulic model, thus allowing to drastically reducing the topographical data of river cross-sections; (2) the procedure for Manning's coefficient calibration allowed to get high performance of the hydraulic model just considering the

HESSD

8, 2699–2738, 2011

observed water levels and sporadic measurements of maximum surface flow velocity during the rising limb of flood. Indeed, in terms of errors in magnitude on peak discharge, for the optimal calibration, they were found, in average, not exceeding 5% for all events observed in the three investigated gauged sections, while the Nash-Sutcliff efficiency was, in average, greater than 0.95. Therefore, the proposed procedure, apart from to have turned out reliable for the rating curve assessment at ungauged sites, can be applied in realtime for whatever flood conditions and this is of great interest for the practice hydrology seeing that, looking at new monitoring technologies, it will be possible to carry out velocity measurements by hand-held radar sensors in different river sites and for the same flood.

1 Introduction

A fast and accurate estimation of the discharge flowing river sections is of great interest for a large number of engineer-ing applications such as real time flood forecasting and water resources management. Therefore, the rating curve knowledge at a river site is fundamental to this aim. It is well known that a rating curve is based on the indirect measure of discharge which is tied to the mean flow velocity inferred through the sampling of velocity points by current meter in the flow area. However, during high floods at a gauged river section, standard velocity measurements are difficult and particularly dangerous for operators, because velocity points cannot be sampled in the lower portion of the flow area. On the other hand, the value of maximum flow velocity can be more easily obtained since its position is located in the upper portion of the flow area where velocity measurements can be easily carried out also during high flow conditions (Chiu, 1987). Based on this insight, many studies have addressed the spatial velocity distribution (Fulton and Ostrowski, 1970; Chiu, 1988; Sulzer et al., 2002) of the flow section and the entropy theory (Shannon, 1948) has been successfully applied for the reconstruction of the solid of velocity starting from the sampling of maximum flow velocity only. A first analytical entropic characterization of velocity profiles can be found in the Chiu's works (1988; 1989), who proposed an algorithm for the estimation of the

HESSD
8, 2699–2738, 2011

two-dimensional velocity distribution in the flow area. The algorithm, however, for practical applications is onerous in terms of parameters estimation and for that simplified entropic approaches have been developed by reducing the model complexity and the errors in mean flow velocity estimation (Chiu and Said, 1995; Moramarco et al., 2004). This insight, i.e., to monitor discharge just by sampling the maximum flow velocity, is of great interest for the practice hydrology, seen that the new technology for the streamflow monitoring is addressed to surface velocity measurements by using equipments like radar sensors (Plant et al., 2005; Costa et al., 2006; Fulton and Ostrowski, 2008).

Therefore, based on the above insights and on the premise that installation of a water level gauge is fairly straightforward and relatively inexpensive, while measurements of velocity are costly, four main configurations of monitoring can be envisaged for a gauged river section. Configuration I; local stages are easily monitored but no velocity measurements are available because the site may be remote and/or inaccessible. Configuration II; like the previous one, with velocity measurements available for low flow depth only. Configuration III; like the first one, with an upstream and/or downstream gauged site with a reliable rating curve. Configuration IV; only local stages are monitored in two hydro-metric sites faraway.

For the first configuration of hydrometric site, the discharge can be indirectly assessed through several approaches based on the Jones formula (Marchi, 1976; Fenton, 1999; Perumal and Moramarco, 2005), used to convert a stage hydrograph to a discharge hydrograph under many unsteady flow situations as well. A comparison of all these approaches can be found in Barbetta et al. (2002) and more recently in Perumal and Moramarco (2005).

For the second configuration, methods as the ones based on the friction-slope factor (Hershy, 1985) can be suitable to extrapolate the rating curve over the velocity measurements field. Limits can be found in parameters assessment mainly during unsteady flow conditions.

The third configuration can be analyzed through approaches estimating the discharge at a given river site by relating the observed local stage to remote discharges

HESSD
8, 2699–2738, 2011

measured at an other upstream/downstream river site (Birkhead and James, 1998; Moramarco et al., 2005). The reliability of these methods is tied to the capability to represent in accurate way the lateral flow along the river reach.

The fourth configuration is referred here as the case of hydrometric stations faraway, where only local stages are meas-ured. In this case, the variable parameter Muskingum stage model such as proposed by Perumal et al. (2007, 2010) and/or hydraulic models more complex as the one by Dottori et al. (2009) and by Arico et al. (2007, 2009) can be applied. In this context, the Arico et al. (2009)'s hydraulic model well lends itself to assess the discharge hydrographs at the upstream section by routing the observed upstream local stages and using for calibrating the Manning's roughness the observed downstream stages. However, the uncertainty in predicting discharge through this model is found to be strictly related to the minimum reach length needed for a good estimation of the celerity of the routed wave. For large peak discharge values, the minimum length can be of the order of several kilometers and significant flow inlets are likely to exist between the two sections.

The paper aim is to improve the discharge hydrograph assessment in the case of Configuration II, when at least one or few instantaneous velocity measurements can be carried out during the rising limb of the flood. To this end, the hydraulic model proposed by Arico et al. (2009), used to compute the discharge hydrograph by routing along a short reach the stages measured at the upstream section, is coupled with the entropic model such as proposed by Moramarco et al. (2004) to asses the mean flow velocity from the information coming from surface flow velocity measurements. The objective is to update the roughness parameter value through hydraulic model calibration by using instantaneous discharge estimated by the entropic model. In addition, the modelled river reach is also investigated whit the aim to estimate the minimum channel length, thus reducing the number of river cross section topographical surveys. Flood events observed in the three gauged river sections along the Tiber River are used for the analysis.

HESSD
8, 2699–2738, 2011

2 Water level driven flow routing

The open channel flow continuity and the momentum equations can be written, neglecting the inertial term, in the following diffusive form:

$$\frac{\partial A}{\partial t} + \frac{\partial q}{\partial x} - Q = 0 \tag{1}$$

$$\frac{\partial H}{\partial x} = -\frac{n^2 q|q|}{A^2 R^{4/3}} \tag{2}$$

where H, A, R, Q, n and q are respectively the water surface level, the cross-section flow area, the hydraulic radius, the lateral inflow, the Manning roughness coefficient and the discharge. The two first order Eqs. (1) and (2) can be merged in one second order equation in the H unknown, that is:

$$\frac{\partial H}{\partial t} - \frac{1}{T}\frac{\partial}{\partial x}\left(\frac{R^{2/3}A}{n}\frac{\frac{\partial H}{\partial x}}{\sqrt{\left|\frac{\partial H}{\partial x}\right|}}\right) = Q \tag{3}$$

where T is the section width.

In order to get a well posed problem, an algebraic function of the surface level H and of its spatial derivatives has to be assigned at each time as known boundary condition in both the initial and the final sections of the domain. Eq. (3) is usually solved using a known discharge hydrograph as upstream boundary condition, that is equivalent to assign the product of the root of the opposite of the surface level gradient time the mean water depth as function of time in the initial section. The management goal of

HESSD
8, 2699–2738, 2011

the model is in this case the computation of the water levels, as function of time and space, in all the downstream sections and also in the initial one.

On the other hand, Eq. (3) can also be solved by giving the observed water levels only as upstream boundary condition. In this case the water level gradient and the corresponding discharge are computed as function of space and time in all the sections, including the initial one.

Previous numerical and laboratory experiments (Arico et al., 2009, 2010) have proved that the downstream boundary condition in the final section can be replaced with an approximated one without any significant effect on the discharge computed in the initial section, if the reach length is long enough. For given reach length, the minimum effect on the computed discharge is obtained setting equal to zero the second order water level derivative at the downstream section. This minimum length has been evaluated using numerical experiments in the order of half the distance between the two hydrometric sites of Configuration IV, as defined in the introduction. In the following section a preliminary criterion for the choice of the minimum reach length, required to get a good discharge estimation at the initial section in the case of Configuration II, will be proposed. The choice of the reach length is important because it has a major impact on the monitoring overall cost, as far as the field survey required for the digital topography reconstruction can not be negligible at all.

2.1 MAST numerical model

Equation 3 is numerically solved in space and time using the MAST technique. The basic idea of the MAST algorithm (Noto and Tucciarelli, 2001; Tucciarelli and Termini, 2000) is to apply a fractional time step procedure to compute the unknown surface level H at time level $k+1$, when the surface level is known at time level k. In the first half-step the predicted level $H^{k+1/2}$ is estimated by integrating in time and space the following prediction equation:

HESSD
8, 2699–2738, 2011

$$\frac{\partial H^{k+1/2}}{\partial t} - \frac{1}{T}\frac{\partial}{\partial x}\left(\frac{R^{2/3}A}{n}\frac{\frac{\partial H^k}{\partial x}}{\sqrt{\left|\frac{\partial H^k}{\partial x}\right|}}\right) = Q \tag{4}$$

In the second half-step the corrected level H^{k+1} is obtained by solving the fully implicit discretization of the following correction equation:

$$\frac{\partial H^{k+1}}{\partial t} - \frac{1}{T}\frac{\partial}{\partial x}\left(\frac{\overline{R^{2/3}A}}{n}\frac{\frac{\partial H^{k+1}}{\partial x} - \frac{\partial H^k}{\partial x}}{\sqrt{\left|\frac{\partial H^k}{\partial x}\right|}}\right) = 0 \tag{5}$$

where the top bar is the symbol of the mean operator, applied along the prediction step. The advantage of splitting the original problem in a prediction plus a correction problem is that these problems can be much easier to solve than the original one.

By applying functional analysis, it can be shown that Eq. (4) is convective and its solution depends on one upstream boundary condition only. After spatial integration, Eq. (4) turns in a system of ordinary differential equations (ODEs). If a further approximation is made and the flux leaving from each computational cell along the time step is approximated with a constant value, the ODEs can be solved sequentially one after the other moving from the cells with higher to the cells with lower water level.

The corrective Eq. (5) is diffusive and its solution depends on both the boundary conditions. After spatial discretization, a fully implicit time discretization is applied to the resulting system. The advantage of solving Eq. (5) instead of Eq. (3) is that the

HESSD
8, 2699–2738, 2011

unknown H^{k+1} can be replaced by the unknown $\eta = H^{k+1} - H^{k+1/2}$. The new variable is small, along with its fluxes, with respect to H^{k+1}. This implies that also the error associated to the fully implicit numerical solution is small with respect to the error in the estimation of the original H^{k+1} unknown. More details on the numerical solution computed using the MAST approach can be found in (Nasello and Tucciarelli, 2005).

3 The flow velocity entropy model: an overview

Moramarco et al. (2004) allowed the estimation of the velocity profile along a vertical by simplifying the two-dimensional velocity distribution introduced by Chiu (1987, 1988, 1989) and based on the entropy theory:

$$u(y) = \frac{u_{\max_v}}{M} \ln\left[1 + \left(e^M - 1\right)\frac{y}{D-h} e^{1-\frac{y}{D-h}}\right] \tag{6}$$

where $u_{\max_v}$ is the maximum velocity sampled along the investigated vertical (Herschy, 1985). M is the entropic parameter, which is a characteristic of the river cross section and can be easily estimated through the linear entropic relation (Chiu and Said, 1995):

$$u_m(y) = \Phi(M) u_{\max} \tag{7}$$

where

$$\Phi(M) = \frac{e^M}{1 - e^M} - \frac{1}{M} \tag{8}$$

Indeed the entropic parameter M can be estimated, for the investigated gauged river site, on basis of pairs $(u_m, u_{\max})$ of available data from measurements sampling (Moramarco et al., 2004). It's necessary to point out that $u_{\max}$ is unknown, but it can be considered as the maximum value in the data set of velocity points sampled during the

HESSD
8, 2699–2738, 2011

velocity measurements (Moramarco et al., 2004). Therefore, once M is estimated at gauged section and $u_{\max_v}$ is sampled in the upper portion of flow area, for instance by current meter, then Eq. (6) can be applied obtaining the velocity profile along each vertical sampled during the velocity measurement. Obviously, the applicability of Eq. (6) depends on the availability of topographical surveys at gauged site which provide the knowledge of the variability of D across the river section. This insight is of great importance if the velocity measurements have to be only addressed in the upper portion of flow area, i.e., during high floods when it is difficult to sample velocity points in the lower portion of flow area. In order to drastically reduce the sampling period during the measurement, we assume that Eq. (6) is applied only considering the maximum velocity point in the flow area, $u_{\max}$, and assuming the behaviour of the maximum velocity quantity in the cross-sectional flow area represented through an elliptical curve (Moramarco et al., 2011):

$$u_{\max_v} = u_{\max}\sqrt{1-\left(\frac{x}{x_s}\right)} \tag{9}$$

where $x_s = x_{sx}$ or $x_s = x_{dx}$ represents the distance from the right or left sidewall of the vertical, with reference to $x = 0$, along which the maximum velocity, $u_{\max}$, is sampled, respectively. Eq. (9) can be derived by Chezy's formula and assuming a depth distribution $\frac{D}{D_{\max}} = 1-\left(\frac{x}{x_s}\right)^2$, with $D_{\max}$ the flow depth along the vertical where $u_{\max}$ is sampled. For narrow river sections, as shown in Moramarco et al. (2004), Eq. (9) should be modified considering a depth distribution raised to power of 1 instead of 0.5, thus obtaining for $u_{\max_v}$ a representation in terms of parabolic curve (Moramarco et al., 2011). It is worth of noting that $u_{\max}$ might occurs on the water surface besides current meter a radar sensor (immovable or hand-held) can be even used for its measure (Fulton and Ostrowski, 2008). In the case $u_{\max}$ occurrs below the water surface and the maximum surface velocity, $u_{\max S}$, can be measured, through Eq. (6) it would be possible to assess $u_{\max}$ as

HESSD
8, 2699–2738, 2011

$$u_{max} = \frac{u_{maxS}}{\frac{1}{M}\ln\left[1+\left(e^{M}-1\right)\delta e^{1-\delta}\right]} \quad (10)$$

where $\delta = \frac{D}{D-h}$ is a parameter easily definable by the velocity sample. Therefore, once the velocity profile have been assessed by Eq. (6), the solid velocity can be computed and, then, the discharge.

4 Proposed domain extension criterion

The main advantage in using a numerical flow routing model for the discharge estimation is that the effect of the topographic error is averaged along the reach extension and the approximation of the adopted downstream boundary condition affects the discharge estimation at upstream end only as much as shorter is the domain extension. However , modelling a long reach, to get the needed topographic information is required. If significant lateral inflows are present downstream the gauged section, their backward effect can also distort the discharge estimation. This implies the need of quantifying with some objective criterion the minimum length that is required to keep small enough the computed upstream discharge error due to the approximated downstream boundary condition.

In the most common case of subcritical flows, the minimum domain extension also depends on the river morphology downstream the end model section, but a rough estimation can be sought after as a function of the main features of the simulated event, according to the assumption of prismatic channel and constant bed slope. These features are the initial water depth inside the channel, the flow depth time derivative at the gauged section, the average Manning coefficient, the bed slope. If we also assume large rectangular section, we can write the diffusive 1-D shallow water equation in the form:

HESSD
8, 2699–2738, 2011

$$\frac{\partial H}{\partial t} - \frac{\partial}{\partial x}\left(\frac{h^{5/3}}{n}\frac{\nabla_x H}{\sqrt{|\nabla_x H|}}\right) = Q \tag{11a}$$

$$H = -ix + h \tag{11b}$$

where $\nabla_x H = \frac{\partial H}{\partial x}$ is the piezometric gradient along x, h is the flow depth and i is the bed slope. We assume very simple boundary conditions, that can be easily assigned in order to overestimate the transition celerity at upstream section. Specifically, at upstream end a linear variation of water depth is surmised:

$$h(0,t) = h_0 + h_0' t \quad \text{with} \quad h_0' = \left.\frac{dh}{dt}\right|_{x=0} = \text{constant} \tag{12a}$$

and at downstream end the kinematic assumption:

$$\frac{\partial H}{\partial x} = -i \tag{12b}$$

According to the upstream boundary condition given by Eq. (12a), the piezometric gradient at $x = 0$ will initially become more negative and then will increase asymptotically toward a finite value equal to the channel bed slope as shown in Fig. 1, wherein, by way of example, for two different lengths, this quantity is plotted. The norm of the difference between its value and the same one computed for $L \to \infty$ will initially rise up to a maximum value, after the maximum of the gradient is attained, and then will tend to zero (see Fig. 1). In order to provide criteria for choosing the minimum channel length as much general as possible, the following dimensionless variables are considered:

$$\begin{cases} \eta = h/L \\ \xi = x/L \\ \tau = \dfrac{t}{nL^{1/3}} \end{cases} \tag{13}$$

HESSD
8, 2699–2738, 2011

Equations (11)–(12) can be written in the following dimensionless form:

$$\frac{\partial \eta}{\partial \tau} - \frac{\partial}{\partial \xi}\left(\eta^{5/3}\frac{\nabla_{\xi}\Psi}{\sqrt{|\nabla_{\xi}\Psi|}}\right) = Q \tag{14}$$

and

$$\eta|_{\xi=0} = \eta_0 + \eta_0'\tau \quad \text{with} \quad \eta_0' = \left.\frac{d\eta}{d\tau}\right|_{\xi=0} \tag{15a}$$

$$\left.\frac{\partial \Psi}{\partial \xi}\right|_{\xi=1} = -i \tag{15b}$$

It is worth to notify that solution η of Eqs. (**??**)–(15) depends, at a given point (η,τ), on parameters i only (in Eqs. **??** and 15b), η_0 and η_0' (in Eq. 15a). If we assume the most severe condition $\eta_0 = 0$, it is $\eta = \eta(i,\eta')$. Observe that parameter η_0' is function of n, because:

$$\eta_0' = h_0'\frac{n}{L^{2/3}} \tag{16}$$

For any occurring upstream flow depth and Manning coefficient, the discharge estimation error is proportional to the error in the gradient root estimation – see Eq. (2). The maximum error, that is the maximum difference between the root of the gradient at $x = 0$ computed with the actual domain length and the same unknown computed using an infinite length, turns out to be:

$$E = \max_t \left| \sqrt{-\nabla_x H_{x=0}\left(n,h_0',i,L,t\right)} - \lim_{L\to\infty}\sqrt{-\nabla_x H_{x=0}\left(n,h_0',i,L,t\right)} \right| \tag{17}$$

HESSD
8, 2699–2738, 2011

and in dimensionless form:

$$E = \max_{\tau} \left| \sqrt{-\nabla_{\xi} \Psi_{\xi=0}\left(n, \eta_0', i, \tau\right)} - \lim_{\eta_0' \to \infty} \sqrt{-\nabla_{\xi} \Psi_{\xi=0}\left(n, \eta_0', i, \tau\right)} \right| \tag{18}$$

Observe in Eq. (16) that the parameter η_0' goes to zero for infinite L, but the limit of the root of the corresponding piezometric gradient in Eq. (20) is different from the trivial value $\sqrt{-\nabla_{\xi} \Psi_{\xi=0}} = \sqrt{i}$ corresponding to $\eta_0' = 0$. This limit can be simply computed using a very large value of L instead of the domain extension used to compute the first gradient in the same Eq. (18). In Fig. 2 the error E of the roots of the upstream piezometric gradient is plotted as function of the dimensionless variable η_0'. Since the limit in Eq. (20) is computed for a finite value of L, the error E is null for a η_0' greater than zero (see Fig. 2). Similar results, obtained by changing the downstream boundary condition given by Eqs. (12b) or (15b) with the following one:

$$\frac{\partial^2 H}{\partial x^2} = 0 \tag{19a}$$

or

$$\frac{\partial^2 \Psi}{\partial \xi^2} = 0 \tag{19b}$$

are shown in Fig. 3.

5 Discharge estimation procedure

Watching Eq. (2), it can be easily inferred that at upstream end, wherein the stage is recorded, $q_{\max}$ is tied to $\sqrt{|\nabla H_{\max}|}$ and n only. Therefore, assuming a semi-infinite channel ($L \to \infty$) and, for that configuration, the water level gradient at upstream end

HESSD
8, 2699–2738, 2011

as benchmark, the error E_d in the estimation of the maximum discharge is given, according to the results of Figs. (2) and (3), by:

$$E_d = \frac{\left| q_{max} - q_{max}^{\infty} \right|}{q_{max}^{\infty}} = \frac{\left| \sqrt{|\nabla H_{max}|} - \sqrt{|\nabla H_{max}^{\infty}|} \right|}{\sqrt{|\nabla H_{max}^{\infty}|}} \leq \frac{E}{\sqrt{i}} \tag{20}$$

where ∇H_{max} and ∇H_{max}^{∞} are respectively the water level gradient corresponding to the maximum discharge computed according to the given reach length and to an infinite reach length. For example, if the measured upstream water level hydrograph reaches the maximum rise of 1 m in 1 h in a channel with $i = 4 \times 10^{-4}$ and $n = 0.04\,\mathrm{m}^{-1/3}\,\mathrm{s}$ and the peak discharge estimation is carried out with a reach length L of about 1000 m, the dimensionless time derivative is, in accordance with Eq. (16):

$$\eta_0' = h_0' \frac{n}{L^{2/3}} = \frac{1}{3600} \frac{0.04}{1000^{2/3}} = 1.11 \times 10^{-7}$$

and the corresponding maximum error (Fig. 2) is about 0.001. The maximum error in the peak discharge estimation obtained adopting the kinematic downstream boundary condition is then equal to:

$$E_d = \frac{E}{\sqrt{i}} = \frac{0.001}{0.02} = 5\%$$

The estimated error is very sensitive to the bed slope. In the previous case, to get en error of only 3% with a slope $i = 10^{-4}$, we need a reach extension of more than 10 000 m. A much smaller extension is required if the bed slope is of the order of 0.1%. In this case, with an extension of 1000 m, we get an error of only 0.7%.

From a practical point of view, Eq. (20) and Figs. 2–3 can be used to assess the minimum channel length so that E_d be less than a fixed threshold. For instance, if E_d was

HESSD
8, 2699–2738, 2011

assigned equal to 5%, then through Eq. (20) it would be possible to compute E. Using Fig. 2 or 3, according to the adopted boundary condition, the curve corresponding to the given i value allow us to infer η'_0 and, hence, by Eq. (16) the optimal value of the channel length, L, for the possible maximum h'_0 and n values.

After a detailed topography data collection, that could call for a computational domain extension (as motivated in the previous section), the numerical model mentioned in section one can be used for the upstream discharge estimation. The hydraulic model is calibrated minimizing the relative absolute error, Err, between the computed, q_{comp}, and observed, q_{obs}, discharge value at time of measure, t_{meas}:

$$\text{Err}(n) = \left| \frac{q_{\text{comp}}(t_{\text{meas}}, n) - q_{\text{obs}}(t_{\text{meas}})}{q_{\text{obs}}(t_{\text{meas}})} \right| \tag{21}$$

wherein $q_{\text{comp}}(t_{\text{meas}}, n)$ is the computed discharge at instant t_{meas} in which the instantaneous surface velocity measurement is carried out by using, for instance, a radar sensor. The simple Brent algorithm (Brent, 1973) is used to find the root of Eq. (21).

6 Performance criteria

The performances of discharge estimation procedure have been evaluated through two criteria (Arico et al., 2009; Perumal et al., 2007) applied to the discharge hydrographs:

1. Nash-Sutcliffe criterion (Nash and Sutcliffe, 1970):

$$NS_q = 1 - \frac{\sum_{i=1,N} \left(q_i^* - q_i\right)^2}{\sum_{i=1,N} \left(q_i^* - \overline{q^*}\right)^2} \tag{22}$$

where q_i^* is the ith data of the benchmark discharge hydrographs, q_i is the ith data of the simulated discharge hydrographs and $\overline{q_i^*}$ is the average value of the benchmark discharge hydrographs.

HESSD
8, 2699–2738, 2011

2. Relative magnitude peak error:

$$\Delta q_p = \left[\frac{q_p}{q_{pM}} - 1\right] \cdot 100 \quad (23)$$

where q_p is the peak value in the computed discharge hydrographs, while q_{pM} is the peak reference value.

7 Field application: the Upper Tiber River

The discharge estimation method, outlined in Sect. 4, has been applied to several flood events occurred along the Tiber River (Central Italy), and recorded at gauged sections of Pierantonio (1800 km^2), Ponte Nuovo (4100 km^2) and Monte Molino (5270 km^2) from December 1996 to December 2010. In the present application the hydraulic model uses the zero-diffusion downstream boundary condition such as given by Eq. (19a). For the investigated sections a reliable rating curve is also available.

At the gauged section of Pierantonio both continuous water level measurements, provided by an ultrasonic sensor, and direct discharge measurements carried out by current meters from cableway, are available. Six flood events, whose main characteristics are reported in Table 1, have been analysed for the methodology testing. The available direct discharge measurements cover almost all the events flow range, except for December 2000 and November 2005, when the flood occupied the floodplains and velocities measurements could not be carried out for the highest water levels (Perumal et al., 2007) These events have been already used by Arico et al. (2009) and Perumal et al. (2007) to validate related discharge estimation methods. The gauged section of Ponte Nuovo is even equipped with ultrasonic flow measurement system (Quantum-Hydrometrie, 2002), which allows to have continuous measurements of both water levels and discharges. In addition, an accurate rating curve is available at site, where velocity measurements are carried out by means of cableway currentmeter. The flood events occurred in November and December 2005 along with December 2008 have

HESSD
8, 2699–2738, 2011

been used as case study (see Table 2). The main flood events characteristics are summarized in Table 2. The gauged section of Monte Molino is object of experimentation of *no-contact* devices for surface water velocity measurement from December 2008, when a fixed radar sensor Sommer RG24$^{(TM)}$ (Sommer, 2002) was installed. More recently at the site was tested a hand-held radar Decatur SVR$^{(TM)}$ (Decatur, 2005). These radar devices have a working frequency of 24 Ghz and a sampling range between 0.3 m s^{-1} to 10 m s^{-1}. Nevertheless both continuous water level measurements, provided by an ultrasonic sensor, and direct discharge measurements carried out by current meters, are available. The flood events occurred in January and December 2010 have been used as case study. The main flood events characteristics are summarized in Table 3.

For the Tiber River including the three investigated gauged sites detailed topographical surveys of cross-sections are available.

7.1 The optimal channel length

With the aim to verify the reliability of synthetic test outcomes, the optimal channel length was computed for each river reach directly below three investigated gauged sections. Surmising a maximum error, E_d, equal to 0.05 for both gauged section, the minimum channel length has been assessed, using the procedure described in Sect. 5. The results of procedure are summarized in Table 4 along with reference quantities for the optimal channel length computation along the three river reaches. In particular for Pierantonio gauged site, in accordance with Eq. (20) the maximum error E has been found 0.019 and a η'_0 value of about 10^{-6} can be inferred by the graph in Fig. 3. Finally assuming a Manning coefficient of 0.048 sm$^{-1/3}$ (Arico et al., 2009) and using the maximum flow depth time derivative observed during the December 2000 event (see Table 1) a minimum channel length, $L_{\min}$, of nearly 45 m for Pierantonio can be estimated by using Eq. (16). Similarly for Ponte Nuovo and Monte Molino sites a $L_{\min}$ values of about 300 m and 50 m is assessed respectively (see Table 4).

HESSD
8, 2699–2738, 2011

The consistency of the minimum channel length obtained for the gauged river site of Pierantonio, according to procedure described in sections 4 and 5 has been tested using the observed flood events there. Fig. 4 illustrates the relative discharge peak error, E_d, obtained by comparing the maximum discharges computed by the hydraulic model assuming different domain lengths, as well as the bed slope and the Manning coefficient reported in Table 4 for the Pierantonio section. The error is computed in comparison with a maximum length of 20.5 km. As shown in Fig. 4, the error E_d is less than 5.5% for all events and greater than 5 % only for events of December 2000 and November 2005, when flooding occurred.

7.2 Discharge hyfdrograph assessment

The analysis presented here is of great interest for the practice hydrology because, in addition to address the discharge monitoring during high floods by coupling the hydraulic model and the entropic one, it would allow to reduce the flow sampling time, so that the discharge can be monitored in different gauged sites for the same flood. Indeed, the entropic model by exploiting the instantaneous velocity measurements, for instance by hand-held radar sensor, can provide the instantaneous discharge value to be used for Manning's calibration. However, we reassert that only at Monte Molino section it has been possible to apply the entropic model, seeing that continuous surface velocity has been observed since December 2008. Save for the site of Ponte Nuovo, where continuous discharge measurements are provided by an ultrasonic flowmeter, the observed discharge hydrographs come from measured water level hydrographs by using the site rating curve.

7.2.1 Pierantonio gauged site

The calibration in terms of Manning's roughness has been carried out at different time along the rising limb of discharge hydrographs, by assuming the observed discharge at that time as benchmark. Related performance have been computed and summarized

HESSD
8, 2699–2738, 2011

in Table 5, for different time of hypothetical sampling along the rising limb. The comparison between the observed discharge hydrographs and the ones obtained by proposed method using a 45 m channel is shown in Fig. 5. As it can be seen, for all events, a good matching between the computed and benchmark hydrographs is obtained when the calibration is carried out in the middle zone of rising limb, where the flood is still developing. For the event December 2000 showing two peaks with discharge values of 389 and 566 $m^3 s^{-1}$, by calibrating at 15th hour, along the first rising limb, the maximum error in peak discharge estimation did not exceed 9% , see Table 5. Notice that the Manning coefficient calibrated at 15th h in the event December 1996 is very close to the optimum one obtained for all other events, except for the one of November 2005, see Table 5, having a peak discharge value about twice the one of December 1996.

7.2.2 Ponte Nuovo gauged site

As above underlined, at Ponte Nuovo site the discharge is even monitored through an ultrasonic flowmeter station. Fig. 6 shows the comparison between the discharge hydrographs coming from the ultrasonic flowmeter and the ones computed through the proposed method, by using for calibration instantaneous discharge values. The performances of calibration and related Manning coefficients are shown in Table 6. As for the previous study case, by calibrating in the middle part of rising limb, the method satisfactory reproduces the discharge hydrograph measured through the ultrasonic flow meter, as shown in Fig. 6. Although the complexity of the two floods due to the flooding occurrence, the main difference can be found only in the upper part of recession limb, showing there a fair matching between the estimated and the observed discharge hydrograph. This is confirmed by the performance measure with error in peak discharge less than 12% for all calibration times (see Table 6).

HESSD
8, 2699–2738, 2011

7.2.3 Monte Molino gauged site

At Monte Molino river site "*no-contact*" method is tested by exploiting the surface flow velocity measurements carried out there by radar sensor. In order to apply the entropic model the parameters M and δ in Eq. (10) were estimated on the basis of available velocity measurements sample and values of 1.77 and 1.33 have been found for them, respectively. Through Eq. (10), u_{max},has been assessed using the observed u_{maxS} and a parabolic distribution of across the flow area, has been considered. Therefore, the entropic model has allowed to assess the instantaneous 2-D velocity distribution by Eq. (6) and then the discharge. For the event January 2010, seeing that the surface flow velocity is available in continuous by Sommer device, it was possible to directly assess by the entropic model the discharge hydrograph as shown in Fig. (7a). As it can be seen a good matching between observed and computed discharge is found. Table 7 shows, besides the flow velocity quantities, the comparison for investigated flood events between the instantaneous discharge computed by the entropic model and the observed ones. The performances of calibrations and related manning coefficients are in Table 8. For the event January 2010 the calibration discharge was computed by using surface water velocity measured by Sommer sensor. Unfortunately this sensor was out of order during the event of December 2010, nevertheless a water surface velocity measurement by means of hand-held Decatur SVR$^{(TM)}$ radar was available in the rising limb of second peak. Besides, calibration points were taken on the rising limb of first peak by using rating curve. Discharge hydrograph obtained by the rating curve is assumed as benchmark in performance computation. Once the Manning coefficient was calibrated, the hydraulic model has been able to satisfactory reproduce the observed discharge as shown in Fig. 7. It is worth of noting that for December 2010, although the entropic model provided an error of about 10% on the instantaneous discharge computation (Table 7), the hydraulic model was able to reconstruct satisfactory the event with an error on the first and second peak that did not exceed 5% and 7%, respectively.

HESSD
8, 2699–2738, 2011

8 Conclusions

Based on the obtained results, the following conclusions can be drawn:

- The analysis on downstream boundary condition effects over the upstream discharge hydrograph computation has shown that short channel lengths are enough to achieve good performance of the diffusive hydraulic model, thus allowing a drastic reduction of the required topographical data of river cross-sections. This insight, however, needs to be further validated in the case of significant irregular sections and bed slopes with respect also to the approximation adopted for the downstream boundary condition.
- The coupling of the hydraulic model with the velocity entropic one turned out of great support for an accurate calibration of Manning's coefficient, allowing us to achieve high performance of the hydraulic model just considering the observed water levels and sporadic measurements of maximum flow velocity.
- The developed algorithm can be conveniently adopted for the rating curve assessment at ungauged sites where only stage are recorded and the standard techniques for velocity measurements fail, in particular during high floods.
- Based on the proposed procedure, discharge hydrographs can be assessed in real-time for whatever flood condition and this is of great interest for the practice hydrology seeing that, by applying the procedure, it will be possible to carry out velocity measurements by hand-held radar sensors in different river sites and for the same flood. A state that never can be realized by using the standard techniques of flow velocity sampling.

HESSD
8, 2699–2738, 2011

References

Arico, C., Nasello, C., and Tucciarelli, T.: Peak flow estimation by means of synchronous water level measurements, in: Proc. of EGU General Assembly, Wien, Austria, 2007. 2703

Arico, C., Nasello, C., and Tucciarelli, T.: Using unsteady water level data to estimate channel roughness and discharge hydrograph, Adv. Water Resour., 32, 1223–1240, doi:10.1016/j.advwatres.2009.05.001, 2009. 2703, 2705, 2714, 2715, 2716

Arico, C., Corato, G., Tucciarelli, T., Mefath, M. B., Petrillo, F., and Mossa, M.: Discharge estimation in open channels by means of water level hydrograph analysis, J. Hydraul. Res., 48, 612–619, doi:10.1080/00221686.2010.507352, 2010. 2705

Barbetta, S., Melone, F., Moramarco, T., and Saltalippi, C.: On discharge simulation from observed stage hydrographs, in: Proc. IASTED International Conference, Crete, Greece, 2002. 2702

Birkhead, A. L. and James, C. S.: Synthesis of rating curves from local stage and remote discharge monitoring using nonlinear Muskingum routing, J. Hydrol., 205, 52–62, 1998. 2703

Brent, R. P.: Algorithms for Minimization Without Derivatives, Prentice Hall, Englewood Cliffs, NJ, 1973. 2714

Chiu, C.: Entropy and probability concepts in hydraulics, J. Hydraul. Eng., 113, 583–600, 1987. 2701, 2707

Chiu, C.: Entropy and 2-D velocity distribution in open channels, J. Hydraul. Eng., 114, 738–756, 1988. 2701, 2707

Chiu, C.: Velocity distribution in open channels flow, J. Hydraul. Eng., 115, 576–594, 1989. 2701, 2707

Chiu, C. and Said, C. A. A.: Maximum and mean velocities and entropy in open-channel flow, J. Hydraul. Eng., 121, 26–35, 1995. 2702, 2707

Costa, J. E., Cheng, R. T., Haeni, F. P., Melcher, N., Spicer, K. R., Hayes, E., Plant, W., Hayes, K., Teague, C., and Barrick, D.: Use of radars to monitor stream discharge by noncontact methods, Water Resour. Res., 42, doi:10.1029/2005WR004430, 2006. 2702

Decatur Electronics Inc.: Surface Velocity Radar (SVR)^{TM} User's manual, Decatur Electronics Inc., Decatur, USA, 2005. 2716

Dottori, F., Martina, M. L. V., and Todini, E.: A dynamic rating curve approach to indirect discharge measurement, Hydrol. Earth Syst. Sci., 13, 847–863, doi:10.5194/hess-13-847-2009, 2009. 2703

HESSD
8, 2699–2738, 2011

Fenton, J. D.: Calculating hydrographs from stage records, in: Proc. 28th IAHR Congress, Graz, Austria, 1999. 2702

Fulton, J. and Ostrowski, J.: Boundary shear distribution in open channel flow, Journal of the Hydraulic Division, 96, 967–994, 1970. 2701

Fulton, J. and Ostrowski, J.: Measuring real-time streamflow using emerging technologies: Radar, hydroacoustics , and the probability concepts, J. Hydrol., 357, 1–10, doi:10.1016/j.jhydrol.2008.03.028, 2008. 2702, 2708

Herschy, R.: Streamflow measurement, Elsevier App. Science Publications, London, UK, second edn., 1985. 2707

Marchi, E.: La propagazione di onde di piena, Atti Accademia dei Lincei, 64, 594–602, 1976. 2702

Moramarco, T., Saltalippi, C., and Singh, V.: Estimation of mean velocity in natural channels based on Chiu's velocity distribution equation, J. Hydrologic Engrg., 10, 58–69, doi:10.1061/(ASCE)1084-0699(2004)9:1(42), 2004. 2702, 2703, 2707, 2708

Moramarco, T., Barbetta, S., Melone, F., and Singh, V.: Relating local stage and remote discharge with significant lateral inflow, J. Hydrologic Engrg., 9, 42–50, doi:10.1061/(ASCE)1084-0699(2005)10:1(58), 2005. 2703

Moramarco, T., Saltalippi, C., and Singh, V.: Velocity profiles assessement in natural channel during high floods, Hydrol. Res., in press, 2011. 2708

Nasello, C. and Tucciarelli, T.: Dual multilevel urban drainage model, J. Hydraul. Eng., 131, 748–754, doi:10.1061/(ASCE)0733-9429(2005)131:9(748), 2005. 2707

Nash, J. and Sutcliffe, J.: River flow forecasting through conceptual models, part 1: a discussion of principles, J. Hydr, 10, 282–90, 1970. 2714

Noto, L. and Tucciarelli, T.: DORA algorithm for network flow models with improved stability and convergence properties, J. Hydraul. Eng., 127, 380–391, 2001. 2705

Perumal, M. and Moramarco, T.: A reappraisal of discharge estimation method using stage hydrographs, in: Proc. HYPESD, vol. I, 104–116, New Delhi, India, 2005. 2702

Perumal, M., Moramarco, T., Sahoo, B., and Barbetta, S.: A methodology for discharge estimation and rating curve development at ungauged river sites, Water Resour. Res., 43, W02412, doi:10.1029/2005WR004609, 2007. 2703, 2714, 2715

Perumal, M., Moramarco, T., Sahoo, B., and Barbetta, S.: On the pratical applicability of the VPMS routing method for rating curve development at gauged river sites, Water Resour. Res., 46, W03522, doi:10.1029/2009WR008103, 2010. 2703

HESSD

8, 2699–2738, 2011

Plant, W., Keller, W., and Hayes, K.: Measurement of river surface currents with coherent microwave systems, IEEE Trans. Geosci. Remote Sensing, 43(6), 1242–1257, doi:10.1109/TGRS.2005.845641, 2005. 2702

Quantum-Hydrometrie: Ultrasonic Flow Measurement System, Berlin, Germany, 2002. 2715

Shannon, C. E.: A mathematical theory of communication, Bell System Tech. J., 27, 379–423, 623–656, 1948. 2701

Sommer, G.: Surface flow velocity – Flow velocity sensor – RG-24, Koblach, Austria, 2002. 2716

Sulzer, S., Rutschmann, P., and Kinzelbach, W.: Flood discharge prediction using twodimensional inverse modeling, J. Hydraul. Eng., 128, 4–54, 2002. 2701

Tucciarelli, T. and Termini, D.: Finite-element modeling of floodplain flows, J. Hydraul. Eng., 126, 416–424, 2000. 2705

HESSD

8, 2699–2738, 2011

Table 1. Maximum benchmark discharge, q_{pM} , maximum measured water level, h_{pM}, peak time water level, t_{ph}, duration and maximum flow depth time derivative, $h_0'\big|_{\max}$, for flood events of the Tiber River at the Pierantonio site.

Event	q_{pM} [$m^3\,s^{-1}$]	t_{ph} [h]	h_{pM} [m]	Duration [h]	$h_0'\big\|_{\max}$ [$m\,s^{-1}$]	Notes
December 1996	380.53	22.5	4.74	49.5	1.39×10^{-4}	
April 1997	429.44	32.5	5.07	74.5	1.94×10^{-4}	
November 1997	308.17	18.5	4.22	45	1.28×10^{-4}	
February 1999	427.93	21.5	5.06	59.5	2.67×10^{-4}	
December 2000	565.89	74	5.92	100	2.39×10^{-4}	Flooding
November 2005	779.03	30.5	7.1	64	2.06×10^{-4}	Flooding

HESSD
8, 2699–2738, 2011

Table 2. As Table 1, but for Ponte Nuovo gauged section.

Event	q_{pM} [$m^3 s^{-1}$]	t_{ph} [h]	h_{pM} [m]	Duration [h]	$h_0' \big\vert_{max}$ [$m s^{-1}$]
November 2005	1073.2	32.75	8.52	70	4.89×10^{-4}
December 2005	804.23	82.16	7.33	115	2.83×10^{-4}
December 2008	874.73	146	7.64	160	3.04×10^{-4}

HESSD
8, 2699–2738, 2011

Table 3. As Table 1, but for Monte Molino gauged section.

Event	q_{pM} [$m^3 s^{-1}$]	t_{ph} [h]	h_{pM} [m]	Duration [h]	$h'_0\|_{max}$ [$m s^{-1}$]
January 2010	1105.2	41.5	9.54	83.5	1.94×10^{-4}
December 2010	995.07	35	8.91	192	1.78×10^{-4}

HESSD
8, 2699–2738, 2011

Table 4. Minimum channel lengths, L_{min}, computed by using a maximum error threshold E_d=5% and a Manning coefficient n=0.048 [$m^{-1/3}s$]. Bed slope, i, root gradient error, E, maximum observed value of $h'_0|_{max}$, $\max\left(h'_0|_{max}\right)$, are also indicated.

River Site	i	E	η'_0	$\max\left(h'_0|_{max}\right)$ [$m\,s^{-1}$]	L_{min} [m]
Pierantonio	1.6×10^{-3}	1.9×10^{-3}	$10^{-}6$	2.4×10^{-4}	45
Ponte Nuovo	0.85×10^{-3}	1.5×10^{-3}	5.3×10^{-7}	4.9×10^{-4}	300
Monte Molino	0.97×10^{-3}	1.6×10^{-3}	7×10^{-7}	1.9×10^{-4}	50

HESSD
8, 2699–2738, 2011

Table 5. Calibration time, t_{Cal}, calibrated Manning coefficients, n, magnitude peak error, q_{pM}, and Nash-Sutcliffe, NS_q, for investigated events at Pierantonio site.

Event	t_{Cal} [h]	n [$m^{-1/3}$ s]	q_{pM} [%]	NS_q
December 1996	12	0.0481	−2.38	0.990
	15	0.0464	1.33	0.999
	20	0.0513	−6.77	0.957
December 1996	22	0.0470	1.73	0.998
	28	0.0470	1.62	0.998
November 1997	5.5	0.0570	−18.87	0.817
	10	0.0475	−2.67	0.995
	12.5	0.0462	0.05	0.998
February 1999	14	0.0480	−0.46	0.994
	15	0.0468	2.32	0.997
December 2000	12	0.0473	6.65	0.990
	14.5	0.0463	8.81	0.982
	63	0.0483	4.24	0.987
November 2003	10.5	0.0487	14.14	0.932
	15.5	0.0481	15.51	0.915
	20.5	0.0522	6.57	0.987
	25.5	0.0546	1.80	0.990

HESSD
8, 2699–2738, 2011

Table 6. As Table 5, but for Ponte Nuovo gauged site.

Event	t_{Cal} [h]	n [$m^{-1/3}\,s^{-1}$]	q_{pM} [%]	NS_q
November 2005	18	0.0401	11.70	0.61
	22	0.0440	1.73	0.88
	24	0.0454	−1.45	0.92
December 2005	17	0.394	11.5	0.94
	74	0.397	11.14	0.95
	76	0.413	6.75	0.98
December 2008	10.5	0.0454	−2.53	0.99
	130.5	0.0429	2.91	0.98
	134.5	0.0426	3.73	0.98

HESSD
8, 2699–2738, 2011

Table 7. Comparison between discharge computed by entropic model, Q_E, and the observed one, Q_{Obs}. Surface velocity, u_{maxS}, maximum velocity, u_{max}, and radar device used for sampling are also tabled.

Event	t_{Cal} [h]	Radar Device	u_{maxS} [m s^{-1}]	u_{max} [m/s]	Q_E	Q_{obs}
January 2010	15		3.25	3.32	682.6	701.7
	20	Sommer RG-24$^{(TM)}$	3.36	3.43	812.1	839.7
	25.5		3.29	3.36	952.8	977.6
December 2010	84.5	Decatur SVR$^{(TM)}$	3.08	3.15	694.1	773.4

HESSD
8, 2699–2738, 2011

Table 8. As Table 5, but for Monte Molino gauged site. Radar device used for surface flow velocity sampling are also reported.

Event	t_{Cal} [h]	Radar Device	n [$m^{-1/3}\,s^{-1}$]	q_{pM} [%]	NS_q
January 2010	15		0.0432	8.43	0.97
	20	Sommer RG-24$^{(TM)}$	0.0445	5.40	0.98
	25.5		0.0457	2.60	0.98
December 2010	17.5	–	0.0411	10.15	0.98
	20	–	0.0421	7.38	0.99
	25.5	–	0.0432	4.76	0.99
	84.5	Decatur SVR$^{(TM)}$	0.0473	−4.43	0.94

HESSD
8, 2699–2738, 2011

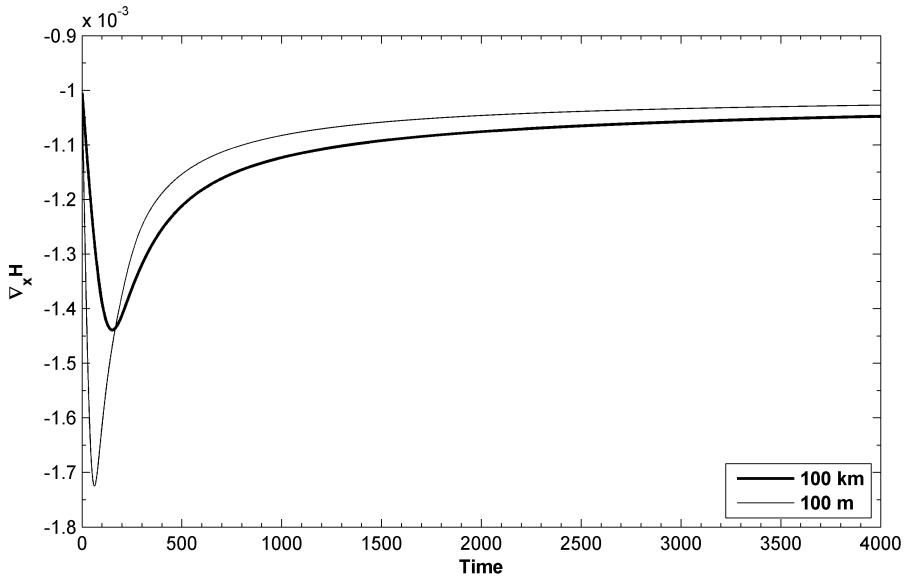

Fig. 1. Example of piezometric gradient, $\nabla_x H$, versus time at $x = 0$ for two channel lengths.

HESSD
8, 2699–2738, 2011

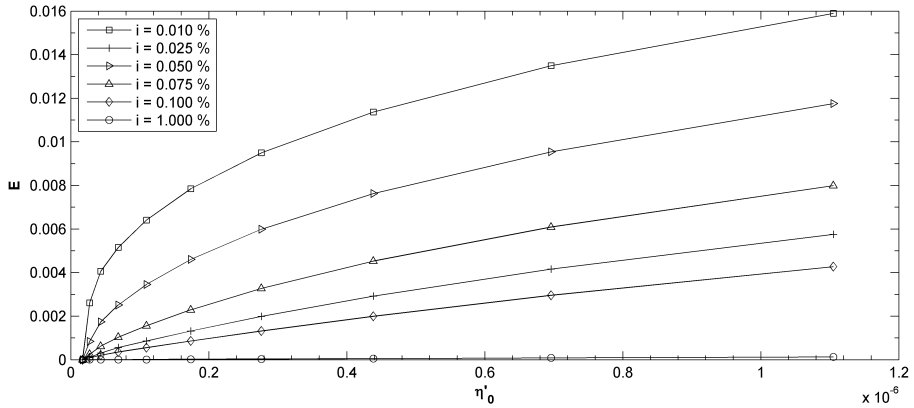

Fig. 2. Root of the gradient norm, E, computed using the boundary condition of Eq. (15) vs. η_0'.

HESSD
8, 2699–2738, 2011

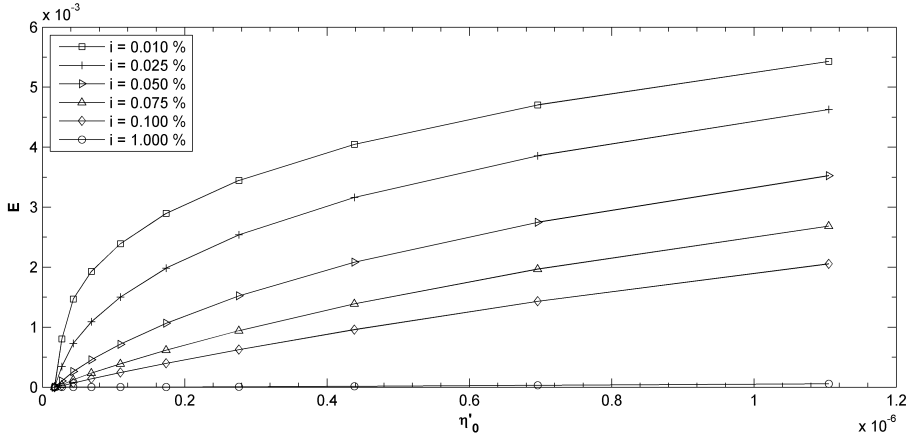

Fig. 3. As in Fig. 2, but for the downstream boundary condition given by Eq. (19).

HESSD
8, 2699–2738, 2011

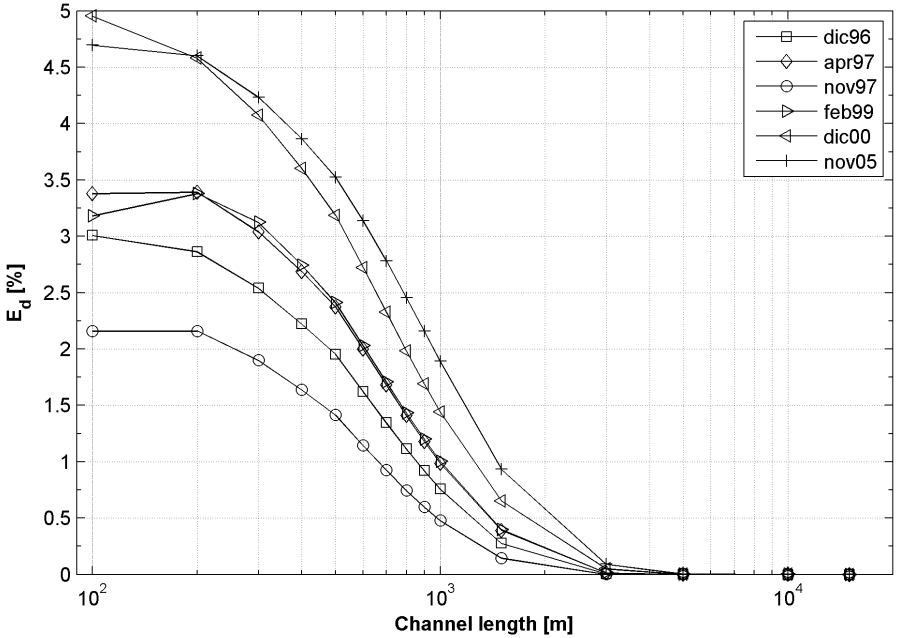

Fig. 4. Pierantonio gauged site: relative discharge peak errors, E_d, versus channel length for analysed events.

HESSD
8, 2699–2738, 2011

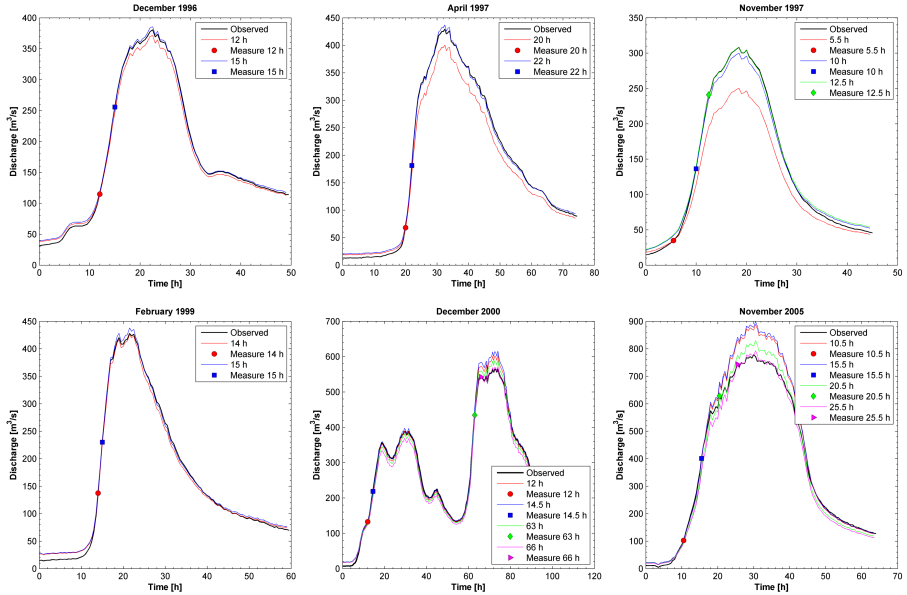

Fig. 5. Comparison between the observed and calibrated discharge hydrographs at the Pierantonio using 45 m channel.

HESSD
8, 2699–2738, 2011

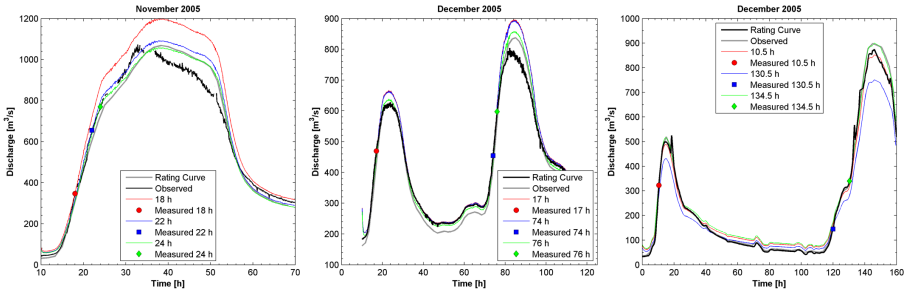

Fig. 6. Comparison between the observed and computed discharge hydrograph at Ponte Nuovo site using a 400 m channel.

HESSD
8, 2699–2738, 2011

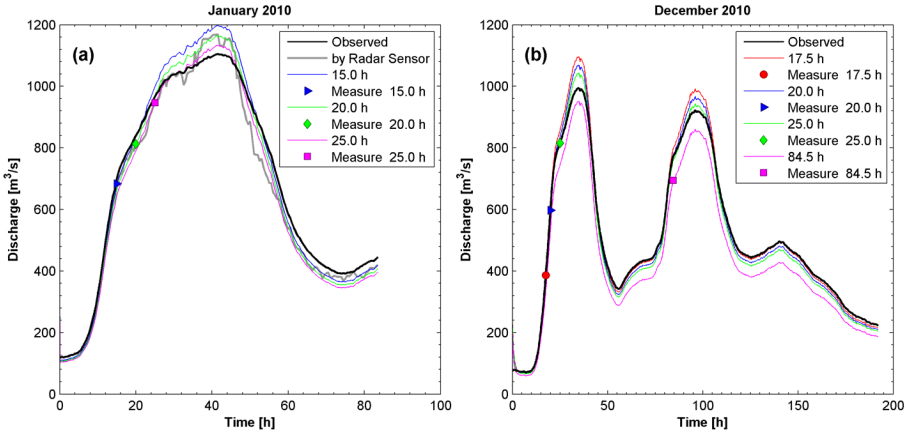

Fig. 7. Comparison between the observed and computed discharge hydrograph at Monte Molino site using a 50 m channel.

HESSD
8, 2699–2738, 2011